ADVANCED THEORY AND SIMULATIONS
www.advtheorysimul.com

Behavioral Posology: A Novel Paradigm for Modeling the Healthy Limits of Behaviors

Nathan Henry, Mangor Pedersen, Matt Williams, and Liesje Donkin*

One of the challenges faced by behavioral scientists is the lack of modeling methodologies for accurately determining when a behavior becomes problematic. The authors propose "behavioral posology" as a novel modeling paradigm for quantifying the healthy limits of behaviors through the concept of behavioral dose. As an example of this paradigm, a pharmacokinetic/pharmacodynamic model of a hypothetical digital behavior is presented, based on opponent process theory. The generic model can be adapted to simulate Solomon and Corbit's model of affective dynamics from 1974, and the model predicts features of addiction such as hedonic allostasis, withdrawal, and apparent tolerance. A behavioral frequency response analysis (BFRA) of the model demonstrates how behavior repetition may result in a hormetic dose–response relationship that depends on the frequency of the behavior. The model can be experimentally validated using Ecological Momentary Assessment, allowing researchers to hypothesize, model, and test causal mechanisms for behavioral addictions. The potential for behavioral posology to be applied as a clinical support tool in psychological medicine is discussed, as this modeling framework may help to detect and limit behaviors being performed too frequently based on factors such as the person's moral beliefs.

1. Introduction

1.1. Rationale for Behavioral Posology

Posology is the study of dosage. It is mainly used for optimizing therapeutic drug administration, but has also been used to establish safe doses for illicit drugs in therapeutic contexts, such as cannabis[1,2] and LSD (lysergic acid diethylamide).[3] Evidence suggests that behavioral and drug addictions have a similar etiology,[4–7] indicating that a posological paradigm could be applied to study the temporal nature of behavioral addictions—particularly those of a digital nature.

Many mental health disorders have been linked to the excessive use of technology. Examples include increased rates of depression and anxiety in high users of social media,[8] smartphones,[9] gaming,[10] pornography,[11–15] and Internet-related behaviors in general.[16] Still, there is debate over whether behaviors such as compulsive pornography use can be classified as addictive, due to insufficient evidence of causal directionality between the behaviors and their associated mental states.[17–20]

Some causal mechanisms for depression induced by repeatable behaviors have been proposed. For example, correlational studies show that people who morally disapprove pornography but continue to use it experience greater levels of depression, anxiety, and distress.[21–24] Moral incongruence can be defined broadly as the feelings of distress, guilt and shame experienced when one performs a behavior that violates one's moral code.[21] Lewczuk et al.[24] highlighted the potential role of moral incongruence in self-perceived addiction to the Internet, social networking, and online gaming. Further, Grubbs et al.[22] found that the interaction of behavioral frequency and moral incongruence predicted self-perceived addiction to behaviors such as pornography use and gambling; however, the same has not been found for illicit substances, tobacco, or prescription drugs, and results were inconclusive for alcohol and marijuana use. The authors noted that while context matters, "moral disapproval consistently predicted self-reported addiction to all focal behaviors and substances, with effect sizes in the medium-to-large range".[22] Still, the neuropsychological mechanisms behind this interaction are poorly understood, due in part to a lack of longitudinal data and insufficient causal modeling techniques. In particular, there is no clear method for quantifying whether a person's behavioral pattern has led to long-term mood modification, increased tolerance, or withdrawal—some of the key components of addiction.[5]

This article proposes a novel modeling paradigm called "behavioral posology" to analyze these temporal relationships, in order to find the healthy limits of behaviors. This paradigm may assist researchers in producing causal models of addiction and

N. Henry, M. Pedersen, L. Donkin
Auckland University of Technology
90 Akoranga Drive, Northcote, Auckland 0627, New Zealand
E-mail: nathan.henry@aut.ac.nz
M. Williams
Massey University
Massey University East Precinct Albany Expressway
SH17, Albany, Auckland 0632, New Zealand

The ORCID identification number(s) for the author(s) of this article can be found under https://doi.org/10.1002/adts.202300214

DOI: 10.1002/adts.202300214

has the potential to be applied broadly in the field of behavioral sciences. We demonstrate an example of this method by modeling the relationship between a repeated digital behavior and hedonic states. We also discuss how to validate this model experimentally. But first, we need to explain the historical background of this model.

1.2. Theoretical Background

1.2.1. Opponent Process Theory

Solomon and Corbit's opponent process theory suggests that repeated behaviors can lead to allostasis, a condition where an individual's set point becomes dysregulated and shifts away from homeostatic levels, often leading to a depressed hedonic state.[25] In this theory, the initial euphoric response to a behavior, experience, or drug is known as the "*a*-process". This is followed by a compensatory opposite reaction, or "*b*-process," which consists of a more extended period of negative hedonic state—typically associated with craving and withdrawal—after which homeostasis is restored.[25] Repeating the opponent processes at high frequency prevents recovery to homeostasis due to the slow decay and additive nature of the *b*-process,[25,26] leading to a gradual slide into a depressed mood. While this theory has been broadly accepted, much remains unknown about the psychological and pharmacological mechanisms behind opponent processes.

1.2.2. Pharmacokinetic/Pharmacodynamic Modeling of Opponent Processes

The way the body processes a drug (its pharmacokinetics) and the drug's effect on the body (its pharmacodynamics) can be simulated using pharmacokinetic/pharmacodynamic (PK/PD) modeling. Clinicians use this tool to optimize drug dose regimens.[27] Most PK/PD models rely on the Hill equation to quantify the relationship between a drug's concentration in the body and its pharmacodynamic effects—also known as the biophase curve—which provides a greater understanding of drug–receptor interactions and their effects on mental states.[28,29] A full explanation of the technique is outside the scope of this article, but for those unfamiliar with PK/PD modeling, we recommend Upton and Mould's introductory papers.[30–32]

Opponent process theory assumes that the *b*-process is pharmacokinetically derived from the *a*-process. For example, if the *a*-process is caused by dopamine release, then the *b*-process could be at least partly due to dopamine depletion of equal and opposite magnitude.[33] However, the neurochemical and hormonal cascades for most opponent processes are generally more complex. It's also possible that the dose–effect relationships for the *a*-process and *b*-process could be different, which means different behaviors could lead to varying rates of allostasis and depression based on the Hill equation parameters for the opponent processes generated by the behavior.

In theory, the effect of any chemical or behavioral stimulus on the body can be modeled as a PK/PD process, even for *a*-processes with no opposing after-reaction. For example, laughing or cuddling can produce a pleasurable reaction—due to the release of endorphins and oxytocin—with a negligible opposing response,[34,35] making it near-impossible to observe allostasis. Yet allostasis can still be achieved with very high behavioral frequencies. Laughter-induced syncope, a rare phenomenon where a person can faint from excessive laughter, is an example of this.[36]

Since the *b*-process decays more slowly than the *a*-process, moderators of the *b*-process have the greatest effect on the rate of hedonic allostasis (i.e., the rate at which the subject's mean hedonic state decreases), as shown by Ahmed and Koob's modeling.[37] In another example, Chou and D'Orsogna[33] proposed a link between neuroticism and the *b*-process for certain behaviors, showing that a larger *b*-process produces greater levels of craving, which could lead to addiction. A similar mechanism can be applied to the moral incongruence model of behavioral addiction to simulate a subject's slide into depression via allostasis. From this, a question arises: can we determine the frequency at which any behavior becomes harmful to the user based on their moral beliefs about the behavior? To answer this, we must first understand the concept of hormesis.

1.2.3. Hormesis

Hormesis is a biphasic dose–response relationship where low doses of a stimulus have a positive effect on the organism, while high doses have a negative effect.[38] Numerous examples of hormesis exist in nature,[39,40] medicine, and psychology, such as the Goldilocks zone,[41] the Yerkes–Dodson law,[42] and the therapeutic window.[43] Dose–response curves for toxic substances can be broadly categorized under three models,[44] demonstrated in **Figure 1**:

- Hormesis—low doses are beneficial, but high doses are detrimental beyond a dose threshold, known as the hormetic threshold, or No Adverse Effect Level (NOAEL)
- Linear No Threshold (LNT)—harm increases monotonically with dose
- Linear With Threshold (LWT)—harm increases monotonically with dose, but only beyond NOAEL

1.2.4. Frequency Response Analysis

The hormesis literature generally focuses on the dose–response relationship for single doses.[45] For example, Calabrese has suggested that hormesis is a commonly observed dose–response pattern in addictive drugs, focusing on the relationship between dose concentration and rat locomotor activity.[45] However, this approach may not accurately predict the effects of dose schedules. In their review of hormetic phenomena, Li et al. stated that "the temporal pattern and duration of the exposure are underappreciated factors in determining the net outcome. Intermittent exposure often generates opposite effects as compared to continuous exposure".[46]

In a behavioral context, one should analyze low and high behavioral frequencies to see whether the relationship between behavioral frequency and effect is linear (e.g., LNT) or nonlinear (e.g., LWT or hormesis). This can be assessed using frequency

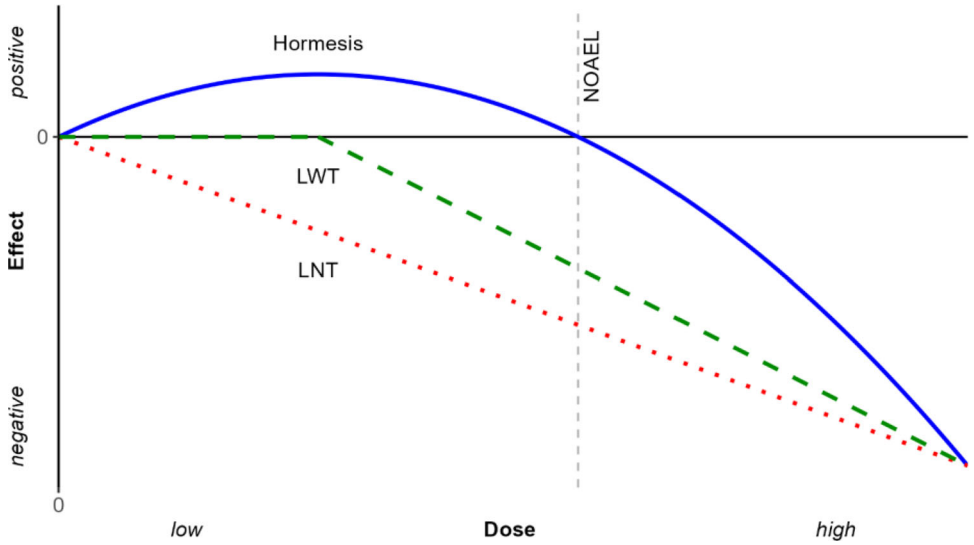

Figure 1. Generic graphs of the Linear No Threshold model (LNT, dotted line), Linear With Threshold model (LWT, dashed line), and hormesis (solid line) for both drug-based and behavioral contexts. NOAEL = no adverse effect level (also known as the hormetic threshold), presented for the hormetic curve only.

response analysis (FRA), a signal processing technique that involves creating Bode plots to show a system's response to inputs of different frequencies.[27] This method has already been applied in biological contexts. Schulthess et al. proposed that dosing frequency could be modulated to affect the pharmacodynamic response and demonstrated four pharmacological problems where FRA could be used to optimize drug treatment regimens.[27] Mitchell et al. discovered an optimal frequency of oscillation for a mitogen-activated protein kinase signaling network in yeast; above and below this frequency, the response was dampened.[47] Radiotherapy is another field in which the frequency of radiation dose delivery significantly impacts therapeutic outcomes.[48]

We propose that one can observe hormesis in behaviors by changing their frequencies and observing the hedonic outcomes, as part of a behavioral frequency response analysis (BFRA). Assuming a hormetic relationship, positive long-term hedonic outcomes will be observed at low behavioral frequencies, but negative long-term outcomes will occur at higher frequencies. Therefore, one can use a BFRA to identify the behavioral frequency range that produces positive long-term hedonic outcomes for individuals.

1.2.5. Modeling "Behavioral Dose"

Using a "black box" approach, it is possible to infer a drug's properties by evaluating its effects on a person's mental state over time. In other words, one can reverse engineer the pharmacokinetics of a drug—how the body processes it—from its pharmacodynamic effects on the brain.[32,49–51] This approach is used when it is too difficult to measure the underlying biological mechanisms of a drug.[52] Similarly, it may be possible to use this approach to understand the effects of performing a behavior on one's mental state.

To do this, behavioral "dose" must first be defined. A concept analysis by Manojlovich and Sidani[53] found that four attributes can describe the "dose" of an intervention: purity, amount, frequency, and duration.[54,55] By reframing "intervention" as "behavior"[56] and "purity" (i.e., concentration) of dose as "potency" of the behavior,[57] we can similarly define behavioral dose. For example, "video gaming dose" can be determined by recording the following metrics:

- *Potency*: the level of immersion or engagement in the behavior (e.g., a game played on a high-end gaming console is likely to provide greater immersion than the same game played on a smartphone)
- *Amount*: the time spent performing the behavior (e.g., length of a gaming session)
- *Frequency*: how often the behavior is performed within a specific period (i.e., *Duration*).

Then, the gaming dose for a single session can be calculated as follows:

$$Dose_{individual\ session} = Potency \times Amount \tag{1}$$

and the total dose of cumulative gaming sessions within a specific period is:

$$Dose_{total} = Frequency \times Duration \times \overline{Dose_{individual\ sessions}} \tag{2}$$

where $\overline{Dose_{individual\ sessions}}$ represents the mean individual session dose for all gaming sessions over the duration in which $Dose_{total}$ is assessed.

Thus, we can perform a BFRA by treating *Potency*, *Amount*, and *Duration* as constants and replacing *Dose* with *Frequency* on the *x*-axis of Figure 1. However, this definition is problematic because it implies a fixed effect, when in fact the effect of behavior on one's mental state varies over time. It also does not capture the complexity of multiple behavioral doses applied in rapid succession. To better model the cumulative effects of repeated doses,

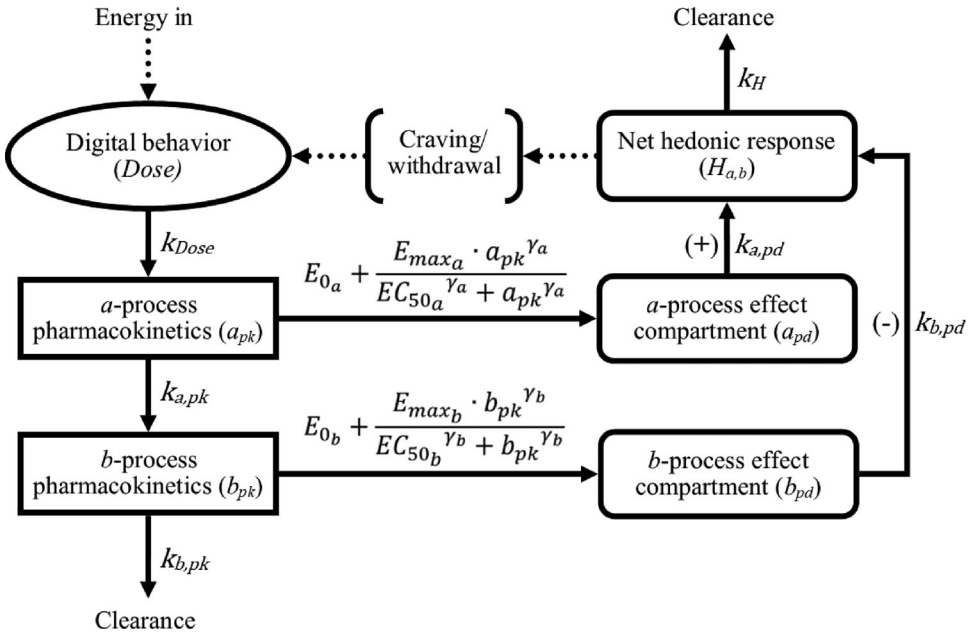

Figure 2. Hypothesized compartment model representing the cycle of a repeated digital behavior, potentially leading to addiction. Compartments linked by dotted lines were not modeled but demonstrate how the cycle of addiction could continue.

a PK/PD model of the opponent processes generated by each behavioral session could be created and validated using experimental data.

1.3. Conclusion

It may be possible to detect healthy limits for certain behaviors, by changing the frequency of behavioral doses and observing the effects on a person's mental state. This type of analysis can be performed using a modeling paradigm called behavioral posology. In this article, we will define behavioral posology and demonstrate its use by performing a BFRA on a hypothetical digital behavior to determine the healthy limits of that behavior. We will also discuss how this model can be tested experimentally using an Ecological Momentary Assessment (EMA) study.

2. Experimental Section

2.1. Mathematical Model

This work created a proof-of-concept PK/PD model of a digital behavior to simulate Koob and Le Moal's conceptual framework of allostasis, based on Solomon and Corbit's theory of opponent processes.[25] The *mrgsolve* package (v1.0.9) in R v4.1.2[58,59] was used to code the model as a system of ordinary differential equations (ODEs). The base model (**Figure 2**) was a two-compartment pharmacokinetic model with zero order infusion (i.e., the behavioral dose directly induced a change in hormonal states, with no intermediate processing) and had a hedonically positive *a*-process. The model code is available in the supplementary materials. The following assumptions were made, based on the principles of affective neuroscience and opponent process theory:[25,26,60]

- A behavior results from a stimulus that creates a desire for a state change.
- Conservation of energy and mass is observed, meaning that the pharmacokinetic concentrations of the *a*- and *b*-processes are linked.
- A neurochemical and hormonal response cascade at least partially drives the emotional response to this state change. An approximate model of the behavior's effects doesn't require perfect knowledge of the sequence of hormones released.
- The initial *a*-process is followed by an oppositional *b*-process, which is caused by the depletion of the *a*-process hormones or the release of other hormones in response to the *a*-process.
- Behaviors have a complex relationship with internal and external events, which can generate either a positive or negative net hedonic outcome. For example, using social media to plan an activity with friends can promote long-term social bonding and generate a greater positive response than negative, resulting in a net positive outcome—despite the possibility that the person may feel some cravings for social media use afterward.

In Figure 2, the PK compartments are the first to follow the *Dose* compartment, and these represent the concentrations of neurochemicals and hormones released into the brain and bloodstream following the digital behavior. The PD (or "effect") compartments represent the intensity of the neurochemicals' effects on the body, for both the *a*- and *b*-processes.[61] The relationship between the PK and PD compartments is governed by the Hill equation. The value of the "net hedonic response" compartment is calculated as the sum of the opposing *a*- and *b*-process PD compartments and represents the brain's overall perception of the person's mood, or the "manifest affective response".[25] For simplicity, each compartment was treated as a discrete location within the body. While multiple brain regions are likely to be involved in hedonic states, our model of opponent processes did

not require these regions to be treated separately to produce useful results.

The equations for the base model are listed below. Due to the hypothetical nature of the model, arbitrary units were used for most variables, unless stated otherwise:

$$\frac{dDose}{dt} = -k_{Dose}Dose \tag{3}$$

$$\frac{da_{pk}}{dt} = k_{Dose}\ Dose - k_{a,pk}a_{pk} \tag{4}$$

$$\frac{db_{pk}}{dt} = k_{a,pk}\ a_{pk} - k_{b,pk}b_{pk} \tag{5}$$

$$\frac{da_{pd}}{dt} = E_{0_a} + \frac{E_{max_a}\cdot {a_{pk}}^{\gamma_a}}{{EC_{50_a}}^{\gamma_a} + {a_{pk}}^{\gamma_a}} - k_{a,pd}a_{pd} \tag{6}$$

$$\frac{db_{pd}}{dt} = E_{0_b} + \frac{E_{max_b}\cdot {b_{pk}}^{\gamma_b}}{{EC_{50_b}}^{\gamma_b} + {b_{pk}}^{\gamma_b}} - k_{b,pd}b_{pd} \tag{7}$$

$$\frac{dH_{a,b}}{dt} = k_{a,pd}\ a_{pd} - k_{b,pd}b_{pd} - k_H H_{a,b} \tag{8}$$

where t is the time elapsed, in minutes; *Dose* is the compartment for hormonal and neurochemical concentrations following digital technology use; a_{pk}, b_{pk}, a_{pd} and b_{pd} are the pharmacokinetic (*pk*) and pharmacodynamic (*pd*) compartments for the *a*- and *b*-processes; k_{Dose}, $k_{a,pk}$ and $k_{b,pk}$ are the clearance rates for the pharmacokinetic compartments; $k_{a,pd}$, $k_{b,pd}$ and k_H are the clearance rates for the pharmacodynamic compartments; E_0, E_{max}, EC_{50} and γ are the coefficients of the Hill equation governing the shape of the biophase curve and the relationship between PK and PD, where E_0 represents baseline effect, E_{max} represents the maximum possible effect, EC_{50} represents half-maximal effect, and γ is the sigmoidicity parameter describing the steepness of the biophase curve; and $H_{a,b}$ is the hedonic response compartment. At time $t = 0$, the values of the compartments were set as follows: $Dose\ (0) = 1$, $a_{pk}\ (0) = 0$, $b_{pk}\ (0) = 0$, $a_{pd}\ (0) = 0$, $b_{pd}\ (0) = 0$, and $H_{a,b}\ (0) = 0$. To simplify the initial model, the clearance rates of the pharmacodynamic compartments ($k_{a,pd}$, $k_{b,pd}$, k_H) were set as constants equal to 1. When $a_{pd} > b_{pd}$, the manifest affective response was denoted as the A-state, and when $a_{pd} < b_{pd}$, the response was denoted as the B-state.

Solomon and Corbit's 'hedonic scale' of affect[25] was used as the primary outcome variable, with a value of 0 representing a neutral mood. The pharmacodynamic effects of the behavior were described as transit compartments following their pharmacokinetic compartments. Input dose was distributed over a variable length of time, known as the infusion time, or time during which the behavior was performed. The initial model had a 1-min infusion time, which was near-instantaneous on the timescale used. To achieve a steady-state response at each behavioral frequency, $Dose_{individual\ session}$ constant was kept for each simulation. This allowed to perform a BFRA that focused purely on the effects of modifying *Frequency*.

Parameters were arbitrarily chosen to mimic the exponential decay of dopamine release and clearance in the brain as measured and modeled by Everett et al.[62] and Chou and D'Orsogna.[33] The Hill equation was adjusted for both *a*- and *b*-processes so that the relationship between dose and effect for both processes was approximately linear for most of the plausible range of dose concentrations. A high ratio of PK:PD magnitudes was chosen to simulate realistic opponent process dynamics, but other parameter sets would likely achieve similar dynamics. The main interest was how the *a*- and *b*-process influenced hedonic outcomes, not the PK-PD relationship. Therefore, $k_{a,pd}$, $k_{b,pd}$ and k_H were set as constants equal to 1, and the pharmacokinetic clearance rates (and EC_{50_b}) were only hanged to adjust the *a*- and *b*-process magnitudes.

γ_b was set to 2, representing positive cooperativity, to produce allostatic effects and apparent tolerance without requiring a feedback loop. The Hill equation for the *a*-process was relatively insensitive to the γ_a parameter, due to the size of $E_{\max a}$. Hence, both the *a*-process and *b*-process were treated as having identical γ values. However, the pharmacokinetic compartment for the *b*-process (b_{pk}) had a slower evolving curve because it had a lower clearance rate than the *a*-process (i.e., $k_{b,pk} < k_{a,pk}$).

In simpler terms, the model was designed to simulate a hypothetical dose of a digital behavior that generates a short, intense burst of pleasure-inducing hormones during the behavior and a longer period of decreased hormone release and increased craving after the behavior ends. This response cycle has a shorter, more intense *a*-process than Koob and Le Moal's model,[26] which is plausible for behaviors such as pornography and social media use, where the *a*-process has a short duration, while the *b*-process is likely to be longer and less intense.

The model was optimized to predict short- to medium-term hedonic outcomes over a range of days. For this reason, this work did not include the "Craving/withdrawal" compartment in the model, which would have turned this into a stochastic closed-loop model[33,51,63] Instead, for simplicity, net hedonic effects were calculated at constant behavioral frequencies, replacing the "Craving/withdrawal" compartment with a constant frequency input to the *Dose* compartment.

2.2. BFRA of PK/PD Model

The model was run across a range of dose frequencies as part of a BFRA. For a single behavioral dose initiated at time $t = 0$, the integral of the hedonic compartment over time, $H_{a,b}(t)_{single}$, can be calculated; this represents the sum of mood scores produced by the behavior over the time of the simulation t_{sim}, and indicates whether the behavior had a net positive or negative hedonic effect on the individual:

$$\int_0^{t_{sim}} H_{a,b}(t)_{single}\ dt = \int_0^{t_{sim}} \left(\frac{k_{a,pd}a_{pd}\ (t) - k_{b,pd}b_{pd}\ (t) - \frac{dH_{a,b}(t)}{dt}}{k_H} \right) dt \tag{9}$$

If multiple behavioral doses are added at a constant frequency, the opponent processes can be summed to find the total integral for $H_{a,b}(t)_{total}$:

$$\int_0^{t_{sim}} H_{a,b}(t)_{total}\ dt = \sum_{i=0}^{n} \int_{i/f}^{t_{sim}} \left(\frac{k_{a,pd}a_{pd,i}(t) - k_{b,pd}b_{pd,i}(t) - \frac{dH_{a,b,i}(t)}{dt}}{k_H} \right) dt \tag{10}$$

where n is the number of behavioral doses added to the initial dose at a frequency f during t_{sim}; therefore i/f is the infusion start time of the new behavioral dose i. A Bode magnitude plot can then be plotted to show the system's frequency response, in terms of the magnitude of $\int_0^{t_{sim}} H_{a,b}(t)_{total}\, dt$ as a function of f. Unlike a typical Bode plot, since the opponent process is not a sinusoidal function, phase does not require analysis.

Allostasis occurs when the *b*-processes accumulate without sufficient recovery time. Hence, the simplest (and most plausible) way to change the rate of allostasis was to modify the Hill equation for the *b*-process, particularly EC_{50_b} and $E_{\max_b}$ which have been associated with tolerance development in drug addiction.[64,65] To simplify the model, EC_{50_b} was only modifiedto simulate a change in moral incongruence, which in turn adjusted the rate of allostasis.

3. Results

3.1. Initial Model

Figure 3 shows the compartment values for a_{pk}, b_{pk}, a_{pd}, b_{pd}, and $H_{a,b}$ at a dose frequency of 0.006 min^{-1}, for $k_{Dose} = 10, k_{a,pk} = 0.02, k_{b,pk} = 0.004, k_{a,pd} = 1, k_{b,pd} = 1, k_H = 1, E_{0_a} = 0, E_{max_a} = 1, EC_{50_a} = 1, \gamma_a = 2, E_{0_b} = 0, E_{max_b} = 1, EC_{50_b} = 3$ and $\gamma_b = 2$. Dose infusion time was set to 1 min, while t_{sim} was set to 1000 min. Since $EC_{50_b} > EC_{50_a}$, the biophase curve is shifted to the right for the *b*-process (Figure 3b), which results in a net positive score for $\int_0^{t_{sim}} H_{a,b}(t)_{single}\, dt$, since the *a*-process is greater than the *b*-process. However, at higher dose frequencies, $\int_0^{t_{sim}} H_{a,b}(t)_{total}\, dt$ has a net *negative* score, because the *a*-processes recover rapidly to baseline levels between behavioral doses, while the summed *b*-processes don't have time to recover due to the longer *b*-process decay time. In other words, opponent processes are generated at time intervals shorter than the critical decay duration of the *b*-process, but longer than the critical decay duration of the *a*-process.[66] This leads to a decreased set point and allostasis. The difference in decay rates can be observed in Figure 3c, which demonstrates buildup for the *b*-process but not for the *a*-process. Consequently, allostasis is observed in Figure 3d.

3.2. Observing Hormesis via BFRA

Figure 4 shows how the three dose–response models (hormesis, LNT, and LWT) in Figure 1 can be produced using a BFRA. We set t_{sim} to 4000 min to allow the *mrgsolve* simulations (Figure 4c,d) to reach steady-state before calculating their integrals. We simulated the moderating effect of moral incongruence on the *b*-process by reducing EC_{50_b} in the Hill equation, indicating that we were treating protective mechanisms that reduce guilt as a reversibly competitive antagonist on the *b*-process.[65] Put simply, by reducing EC_{50_b}, we increased the subject's moral incongruence (their feelings of guilt about the behavior), which in turn increased the magnitude of the *b*-process and raised the rate of allostasis, leading to a more intense hedonic depression. (The darker the curve in Figure 4, the lower the value of EC_{50_b}.) Similar results can also be achieved by changing E_{max_b} (simulating irreversible antagonism) or γ_b (simulating a change in dose sensitivity).[64,65]

BFRA curves for different levels of moral incongruence can be seen in the graph of $\int_0^{t_{sim}} H_{a,b}(t)_{total}\, dt$ (Figure 4e) for varying levels of EC_{50_b}. Lower values of EC_{50_b} shift the biophase curve to the left and generate a larger *b*-process. This increases the rate of allostasis, which becomes visibly observable in the *mrgsolve* simulation (Figure 4c,d) at dose frequencies of 0.001 min^{-1} or greater. Higher values of EC_{50_b} lead to higher hormetic thresholds (i.e., the *x*-intercept of the curve shifts to the right). This indicates that subjects with less moral incongruence are protected against allostasis over a greater range of behavioral frequencies. Put simply, they can perform the behavior more frequently without experiencing excessive guilt or depression.

We used the graph of BFRA curves in Figure 4e to quantify the healthy limits of the digital behavior for each level of EC_{50_b}:

- When $EC_{50_b} = 3.6$, hormesis was observed in the BFRA curve. The behavior could be performed without adverse effects at frequencies below approximately 0.0042 min^{-1} (the hormetic threshold, or NOAEL). Above this frequency, negative total hedonic scores were observed.
- When $EC_{50_b} = 3.0$, hormesis was observed but the hormetic threshold was lower at approximately 0.0026 min^{-1}.
- When $EC_{50_b} = 2.4$, the BFRA curve was similar to the LWT model in Figure 1 (despite some nonlinearity). The behavior could still be performed up to a frequency of approximately 0.0008 min^{-1} before adverse effects were observed.
- When $EC_{50_b} = 1.8$, performing the behavior at any frequency led to adverse effects. This is similar to the LNT model in Figure 1 (despite some nonlinearity).

We can apply this model to a hypothetical real-life scenario. Imagine that a person with a moral incongruence score of $EC_{50_b} = 3.0$ performs the behavior at a frequency greater than 0.0026 min^{-1} (thus exceeding the hormetic threshold). Therefore, the person performs the behavior excessively despite experiencing overall adverse hedonic effects, providing evidence of salience and mood modification. The graphs in Figure 4c,d also demonstrate allostasis beyond the hormetic threshold, providing evidence of tolerance and withdrawal. This suggests that the person may be addicted to the behavior, based on Griffiths' six component model of addiction.[5] However, further examination would be required to confirm that the remaining two components (conflict and relapse) are also present.

3.3. Simulating the "Standard Pattern of Affective Dynamics"

We previously simulated low dose frequencies to leave breaks between doses. This approach was suitable for modeling behaviors with short *a*-processes and refractory periods, such as orgasm during pornography use. However, we wanted to see what would happen if the behavior were performed continuously for an extended period. Such a model could be applied to behaviors of longer duration, such as Internet, smartphone, or gaming

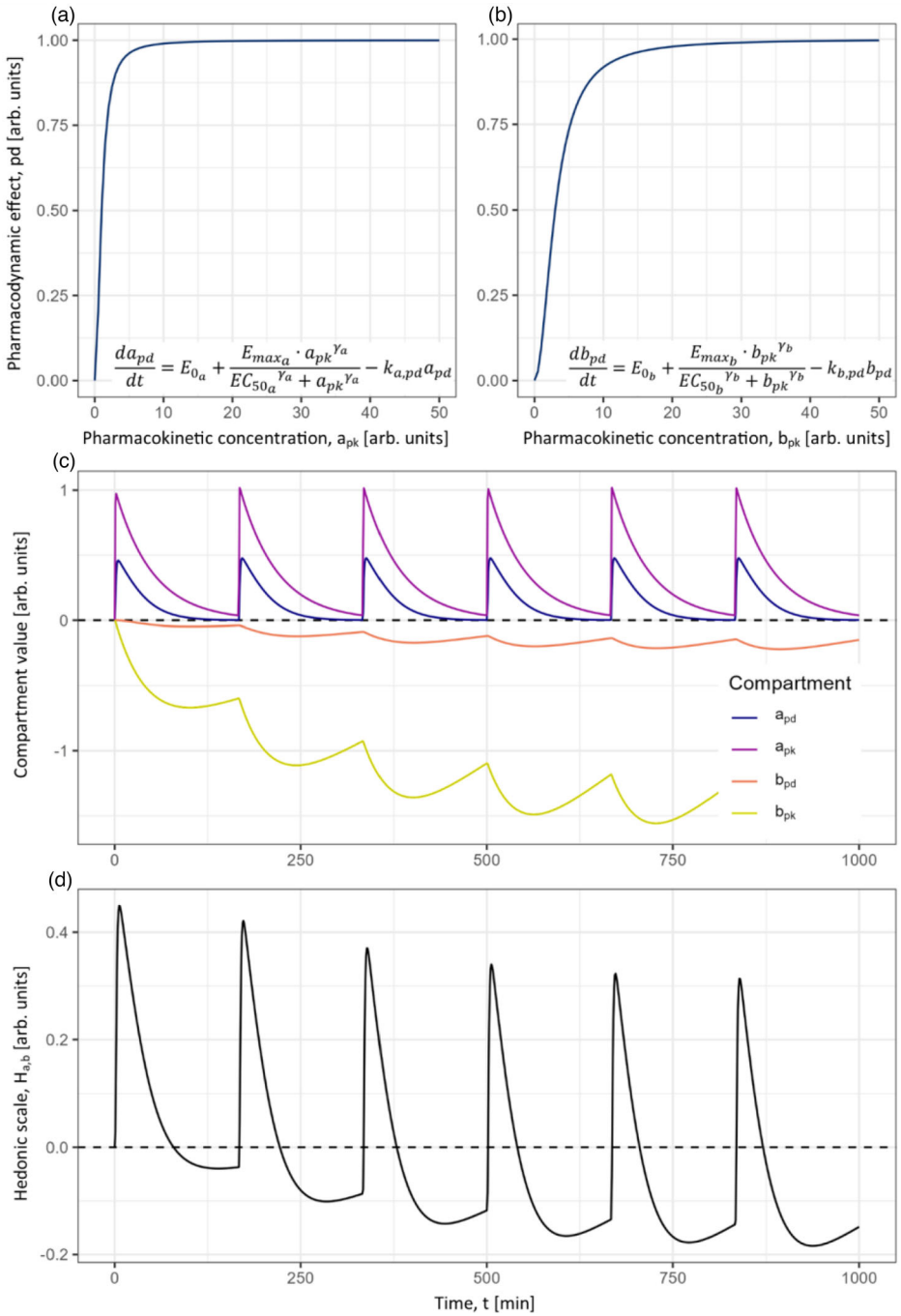

Figure 3. Model showing how summed a- and b-processes can generate an overall decrease in mood (allostasis) over time at high dose frequencies. a,b) Biophase graphs based on Hill equation parameters. c) *mrgsolve*-simulated compartment values for a_{pk}, b_{pk}, a_{pd} and b_{pd}. d) Simulated compartment values for $H_{a,b}(t)_{total}$, showing allostasis and reduced average mood over time.

sessions that last for hours. To do this, we increased the dose frequency to 0.2 min^{-1} (one dose infusion every 5 min) to simulate near-continuous behavioral dosing. At this frequency, the *a*-processes from each individual opponent process didn't have time to fully decay, and the individual opponent processes appeared to merge into a single dynamic process. Remarkably, we observed that at this dose rate, the graph of $H_{a,b}(t)$ closely resembled Solomon and Corbit's "standard pattern of affective dynamics" (Figure 1 of Solomon and Corbit's paper[25]), though on a timescale of minutes rather than seconds.

In **Figure 5**, we demonstrate a simulation of the standard pattern of affective dynamics (dark red, approximating Figure 5 of Solomon and Corbit's paper[25]), as well as the pattern of affective dynamics with tolerance induced by repeated stimulations (light red, approximating Figure 6 of Solomon and Corbit's paper[25]). For both graphs, we set EC_{50_a} to 3 and EC_{50_b} to 35 to reduce the

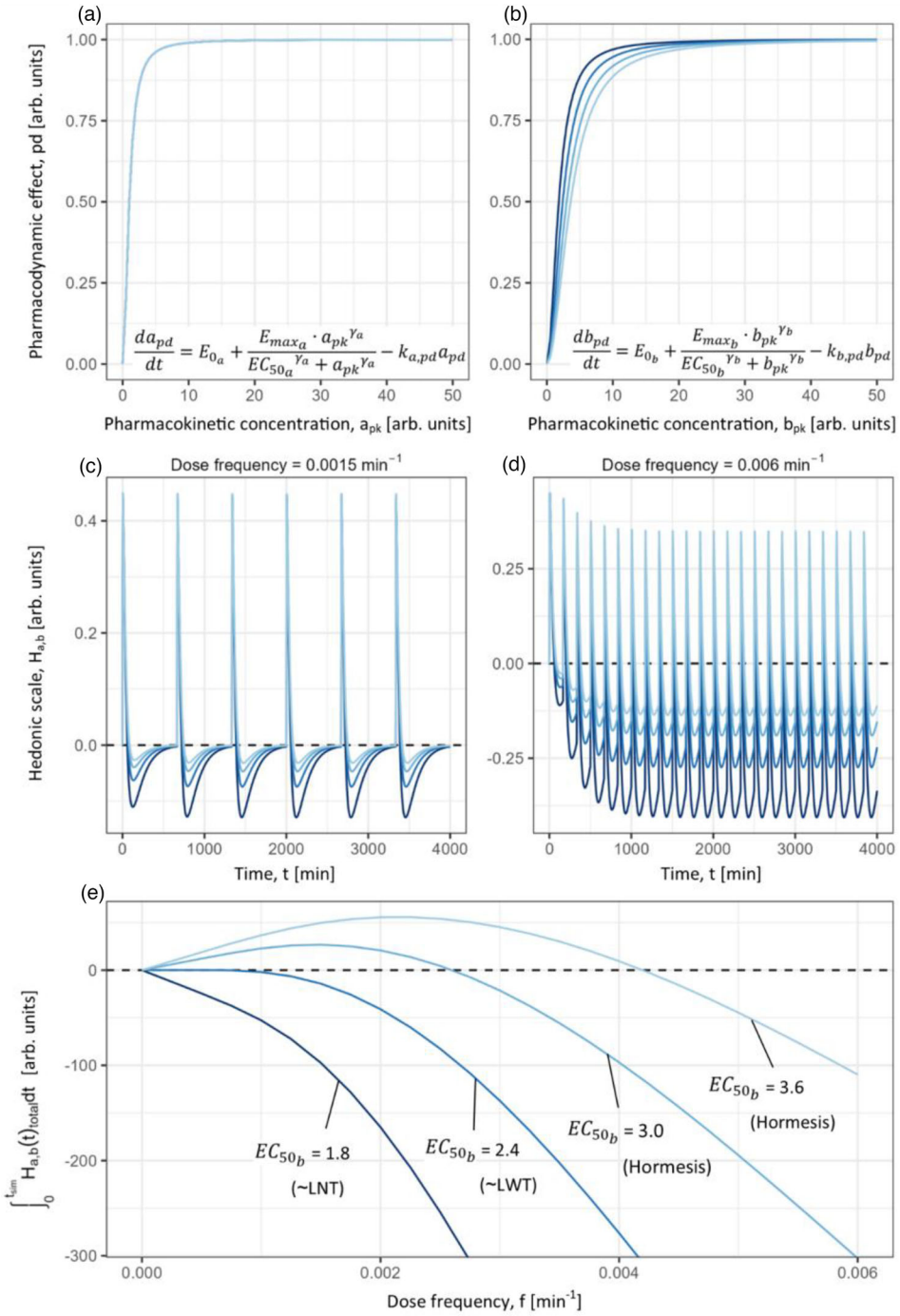

Figure 4. Simulation for varying levels of EC_{50_b} (shades of blue), representing different levels of moral incongruence. a,b) Biophase curves for a- and b-processes. c,d) $H_{a,b}(t)_{total}$ scores generated by *mrgsolve*. At a dose frequency of 0.0015 min^{-1}, b-processes decay to homeostatic levels, but at a higher dose frequency of 0.006 min^{-1}, allostasis is observed at all levels of EC_{50_b}. e) BFRA curves plotted as a function of dose frequency at each level of EC_{50_b}.

b-process magnitude relative to the *a*-process. For the standard pattern, we set $k_{a,pk}$ to 0.02 and $k_{b,pk}$ to 0.005, while for the tolerance-induced pattern, we set $k_{a,pk}$ to 0.04 and $k_{b,pk}$ to 0.004, increasing the decay rate of the *a*-process and decreasing the decay rate of the *b*-process. We ended dose input after 300 consecutive doses to observe withdrawal effects. As behavioral frequency increased, the hedonic state converged to an equilibrium value before the dose was withdrawn (Figure 5d). Five distinct phases are observed in both graphs, which can now be explained as follows:

1) The peak of the primary affective reaction (A-state): represents the cumulative effects of the *a*-processes from each behavioral dose.

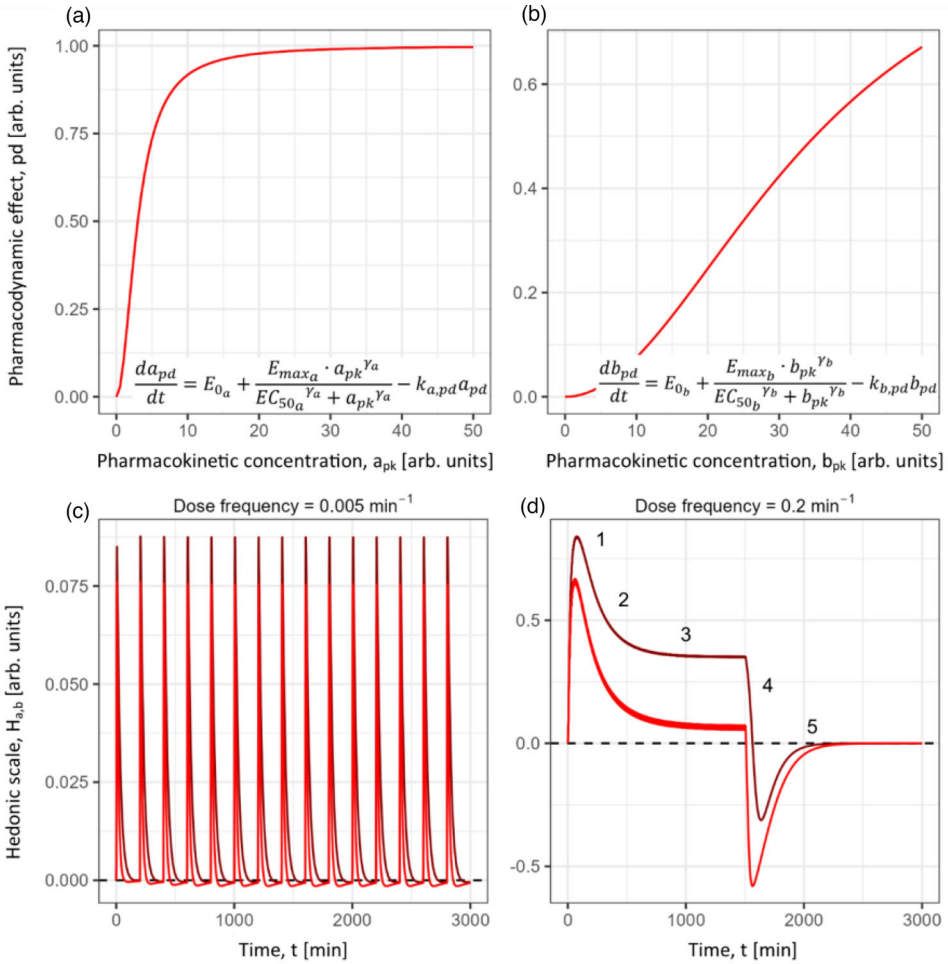

Figure 5. Simulation of Solomon and Corbit's "standard pattern of affective dynamics" (dark red; $EC_{50_a} = 3$, $EC_{50_b} = 35$, $k_{a,pk} = 0.02$, $k_{b,pk} = 0.005$), and tolerance-induced affective dynamics (light red; $EC_{50_a} = 3$, $EC_{50_b} = 35$, $k_{a,pk} = 0.04$, $k_{b,pk} = 0.004$). At a dose frequency of 0.2 min^{-1} (near-continuous dose), the individual opponent processes appear to merge into a single dynamic process, and the graph of $H_{a,b}(t)$ (d) demonstrates the following distinctive features of affective dynamics: peak of primary affective reaction (1), adaptation phase (2), steady-state (3), peak of affective after-reaction (4), and decay of after-reaction (5).

2) Adaptation phase (A-state): the effects of cumulative *b*-processes appear while the *a*-processes start to recover to baseline levels.
3) Steady-state (A-state): equilibrium is reached, with *a*- and *b*-processes generating and recovering at equal rates.
4) The peak of the affective after-reaction (B-state): following removal of the stimulus, the *a*-processes are first to recover, while the *b*-processes take longer to decay, leading to a rapid decrease in hedonic scores. The subject is likely to feel strong withdrawal symptoms during this time.
5) Decay of after-reaction (B-state): finally, the *b*-processes recover to baseline.

These results suggest that the standard pattern of dynamics, as described by Solomon and Corbit in 1974,[25] may be comprised of the sum of multiple opponent processes, with short, intense *a*-processes followed by longer, less intense *b*-processes. However, further experimentation is necessary to confirm this hypothesis.

4. Discussion

4.1. Implications of Behavioral Posology

Behavioral posology is a modeling paradigm for analyzing the cumulative effects of behaviors delivered at varying frequencies, using BFRA. Coupled with empirical data, this approach may enable researchers to accurately predict the effects of performing compulsive behaviors at different frequencies, particularly those involving digital technologies. It also provides a way to quantify the healthy limits of a behavior for an individual, which in turn can be used as one of the criteria for testing whether the individual is addicted to the behavior. This has several clinical implications. For example, behavioral posology could help clinicians treat depressed patients by identifying and limiting problematic behaviors that have exceeded the hormetic threshold. However, to achieve this, experimental studies will be needed to quantify the parameters of the *a*- and *b*-processes of those behaviors so they can be simulated accurately. Future research in this field could

also impact the design of ethical technologies by allowing guidelines to be set for healthy behavioral frequencies, enabling software creators to make more ethical design choices for their apps.

This article also presents four main findings:

1) We support Koob and Le Moal's[37] extension of Solomon and Corbit's[25] model of allostasis by simulating it with an open-loop PK/PD model of opponent processes.
2) As a special case of this PK/PD model, we replicate Solomon and Corbit's "standard pattern of affective dynamics",[25] showing that it can be modeled as the sum of high-frequency, short-duration opponent processes.
3) One can identify behavioral hormesis by altering the frequency of behavior-induced opponent processes and observing the overall impact on the subject, rather than simply studying the effects of a single behavioral dose at different potencies.
4) The width of the hormetic region—i.e., the range of behavioral frequencies that produce a net positive hedonic effect—can be moderated by adjusting the parameters of the PK/PD model, particularly those linked to the *b*-process.

Our PK/PD model has important implications for treating conditions such as depression. For patients who feel guilty about problematic behaviors, reducing the frequency of these behaviors and managing moral incongruence may be key to their treatment. Acceptance and commitment therapy (ACT) can be a practical approach for these cases, as it helps patients to acknowledge negative thoughts and emotions related to their behavior and make changes that align with their values.[67] ACT has already shown promise for treating conditions such as problematic pornography use in multiple studies.[21,68–70] The PK/PD model presented here could be used alongside ACT to determine the healthy limits of these behaviors and assist clinicians in setting goals for their patients.

4.2. Modifying the Model

Thanks to their grounding in neuropharmacological principles, PK/PD models have significant potential for accurately predicting behavioral effects. We have created a simple PK/PD model that can be used as a base model for simulating any behavior with opponent process dynamics. Readers are encouraged to download and modify the R code in the supplementary materials. Simulating other behaviors is as straightforward as running the function "*bode_plot()*" and adjusting the input parameters. Examples of this are provided within the script for the reader's convenience. The *mrgsolve* package is flexible enough to allow for a wide range of customizations, and researchers can estimate parameters empirically to create accurate models for their own field of study.

For example, in the Figure 5 simulation, tolerance to the behavioral stimulus was simulated by increasing $k_{a,pk}$ (shortening the *a*-process) and decreasing $k_{b,pk}$ (lengthening the *b*-process). However, other adjustments were also tested to obtain similar results. For instance, increasing EC_{50_a} (simulating the development of tolerance via a competitive agonist) lowers both the peak of the primary affective reaction and steady-state value, and increases the magnitude of the affective after-reaction. Alternatively, reducing E_{max_a} produces similar effects, as does modifying the clearance rates of the pharmacodynamic compartments ($k_{a,pd}$, $k_{b,pd}$, k_H). (Note that to achieve a positive steady-state, the *a*-process magnitude needs to exceed that of the *b*-process.)

To perform a true BFRA, it is important to keep $Dose_{individual\ session}$ constant for each simulation. However, future experiments should also consider the effects of changing the dose magnitude, perhaps as a function of tolerance development. By changing the ratio of *a*- and *b*-process magnitudes, one can easily adjust the rate of development of allostasis and apparent tolerance. If more sophisticated modification is required, one could add a parallel tolerance compartment to create a feedback loop, similar to those in control system models of addiction in the literature.[32,33,37,51,52,63,71–76] Several types of functional tolerance, both competitive and noncompetitive, could be added, including both pharmacokinetic tolerance (such as changes in metabolite production or transporter function) and pharmacodynamic tolerance (such as modifications to receptor functionality or changes to signal pathways).[52]

4.3. Experimental Validation of Behavioral PK/PD Models

If validated experimentally, our PK/PD model has the potential to explain causal relationships between digital behaviors and mental health metrics. To validate this, longitudinal survey methods such as Ecological Momentary Assessment, or EMA,[77] would be required to capture the temporal dynamics of specific behaviors. An EMA involves regularly sampling an individual's current state, typically by making a participant complete multiple smartphone-based surveys daily.[78] By fitting a PK/PD model to high-frequency EMA data, one could test the hypothesis that allostasis produced by opponent processes can causally predict mental health metrics relative to behavior times. To test for hormesis, the Mack–Wolfe test, a nonparametric rank test for detecting "umbrella" alternatives to monotonic functions, could be performed on the BFRA curves.[79,80] In this way, researchers can use behavioral posology to hypothesize, model, and test causal mechanisms for behavioral addictions.

Our PK/PD model can be run across a range of dose frequencies to perform a BFRA, but only considers constant frequencies. It also focusses on short-term craving and withdrawal effects, which makes it useful only for prediction of hedonic states in the short- to medium-term. While this allows us to perform a more accurate BFRA, it may limit the model's applicability to cases of long-term addiction with a bidirectional relationship between craving and behavioral frequency. Chou and D'Orsogna[33] offer a more comprehensive control-theoretic model of drug addiction by incorporating a craving feedback loop that can accurately simulate the progression to behavioral addiction. A similar feedback loop could be applied to our model, representing the buildup of neural memories that trigger craving and withdrawal symptoms in the long term.

4.4. Future Research

In this article, we focused on hedonic outcomes for a hypothetical digital behavior, using moral incongruence as a moderator of

the *b*-process. However, other moderators could be explored. For instance, one could measure anxiety outcomes due to pornography use as moderated by moral disapproval of pornography,[81] or measure stress outcomes due to social media use as moderated by job characteristics.[82] Furthermore, this type of modeling could be applied to several other fields, such as predicting emotional responses to stock market fluctuations and vice-versa,[83,84] predicting mood outcomes for different styles of music,[85] or predicting marital stability based on positive and negative interactions between partners.[86] We encourage readers to consider whether a behavioral PK/PD model could be helpful in their field of study.

Another possibility lies in the similarity between the shape of the opponent processes modeled in this article (for example, in Figure 4), and the shape of a neuronal action potential. Specifically, an action potential could be characterized as an opponent process, with depolarization being the *a*-process and hyperpolarization the *b*-process. This raises the possibility that the affective states presented in this article could be modeled as the sum of action potentials firing simultaneously in adjacent neurons. Could it be that such an additive mechanism exists within the brain's reward centers? For example, could a person's hedonic state be modeled by the addition of membrane potentials, currents, or even firing rates of neurons within the ventral tegmental area (VTA), an area of the brain involved in reward? Electrode stimulation of brain regions such as the VTA is known to increase the firing rate of neurons in those regions, while simultaneously producing pleasurable hedonic states.[87–91] Other brain regions are also likely to play a role; for example, functional magnetic imaging evidence suggests that the VTA is only indirectly linked to reward magnitude tracking, with neural population activity in the nucleus accumbens being a more reliable correlate of reward magnitude.[92] Yet studies of neural firing within the VTA have shown a pattern in hyperpolarization-activated currents (I_h) where both a "depolarizing voltage sag" and a "repolarizing voltage sag" are observed; these patterns are qualitatively similar to that seen in Figure 5d.[93–96] Future research should investigate whether this indicates a link between the high-frequency firing of action potentials in the brain's reward centers and the "affective dynamics" model, as Figure 5d shows. Such research may improve our understanding of how people perceive hedonic states at a cellular level.

5. Conclusion

Behavioral posology is a modeling paradigm that can be used to analyze the effects of repeatable behaviors on mental wellbeing, and to determine the healthy limits of such behaviors. In this article, we have demonstrated how behavioral posology can be used to model depression induced by repetition of a digital behavior. The model may also provide a causal mechanism for frequency-based hormesis, in which low frequencies of a behavior have some long-term hedonic benefits, but higher frequencies have negative effects on average. This has significant implications for the treatment of behavioral addictions, as it may help clinicians to set goals with greater precision for behavior modification in their patients, in conjunction with a therapy such as ACT. Further research is needed to validate this model empirically across a range of behaviors, which may be achievable using smartphone-based Ecological Momentary Assessments. This article highlights the need for continued development of PK/PD models within the behavioral posology paradigm. We hope that future research in this space will enable us to better predict the healthy limits of behaviors for any individual.

Acknowledgements

The authors would like to thank the reviewers for their perceptive comments. The authors received no financial support for the research, authorship, and/or publication of this article.

Open access publishing facilitated by Auckland University of Technology, as part of the Wiley - Auckland University of Technology agreement via the Council of Australian University Librarians.

Conflict of Interest

The authors declare no conflict of interest.

Author Contributions

N.H. devised and wrote the code for the numerical model, and was the primary author of the manuscript. L.D., M.P., and M.W. supervised and critiqued the modeling process, and contributed to writing the manuscript.

Data Availability Statement

The code that supports the findings of this study is available in the Open Science Framework (OSF) website at https://osf.io/sau4v/, DOI 10.17605/OSF.IO/SAU4V.

Keywords

addiction, allostasis, behavioral addiction, frequency response analysis, hormesis, opponent process, pharmacokinetic/pharmacodynamic modeling

Received: March 25, 2023
Revised: June 1, 2023
Published online: July 3, 2023

[1] V. Giorgi, S. Bongiovanni, F. Atzeni, D. Marotto, F. Salaffi, P. Sarzi-Puttini, *Clin. Exp. Rheumatol.* **2020**, *7*, 53.
[2] G. Lafaye, L. Karila, L. Blecha, A. Benyamina, *Dialogues Clin. Neurosci.* **2017**, *19*, 309.
[3] A. C. Kaypak, A. Raz, *Transcult. Psychiatry* **2022**, *59*, 665.
[4] J. E. Grant, J. A. Brewer, M. N. Potenza, *CNS Spectrums* **2006**, *11*, 924.
[5] M. Griffiths, *J Subst. Use* **2005**, *10*, 191.
[6] G. F. Koob, M. L. Moal, *Philos. Trans. R. Soc., B* **2008**, *363*, 1507.
[7] T. E. Robinson, K. C. Berridge, *Philos. Trans. R. Soc., B Biol. Sci.* **2008**, *363*, 3137.
[8] B. Keles, N. McCrae, A. Grealish, *Int. J. Adolesc. Youth* **2020**, *25*, 79.
[9] J. D. Elhai, R. D. Dvorak, J. C. Levine, B. J. Hall, *J. Affective Disord.* **2017**, *207*, 251.
[10] C.-Y. Wang, Y.-C. Wu, C.-H. Su, P.-C. Lin, C.-H. Ko, J.-Y. Yen, *J. Behav. Addict.* **2017**, *6*, 564.
[11] N. C. Borgogna, R. C. McDermott, *Sex. Addict. Compulsivity* **2018**, *25*, 319.

[12] M. H. Butler, S. A. Pereyra, T. W. Draper, N. D. Leonhardt, K. B. Skinner, *J. Sex Marital Ther.* **2018**, *44*, 127.
[13] C. Harper, D. C. Hodgins, *J. Behav. Addict.* **2016**, *5*, 179.
[14] S. W. Kraus, M. N. Potenza, S. Martino, J. E. Grant, *Compr. Psychiatry* **2015**, *59*, 117.
[15] Y. Okabe, F. Takahashi, D. Ito, *Front. Psychol.* **2021**, *12*, 638354.
[16] M. Brand, K. S. Young, C. Laier, K. Wölfling, M. N. Potenza, *Neurosci. Biobehav. Rev.* **2016**, *71*, 252.
[17] M. Gola, M. Wordecha, G. Sescousse, M. Lew-Starowicz, B. Kossowski, M. Wypych, S. Makeig, M. N. Potenza, A. Marchewka, *Neuropsychopharmacology* **2017**, *42*, 2021.
[18] M. P. Kafka, *Arch. Sex. Behav.* **2014**, *43*, 1259.
[19] R. B. Krueger, *Addiction* **2016**, *111*, 2110.
[20] R. C. Reid, B. N. Carpenter, J. N. Hook, S. Garos, J. C. Manning, R. Gilliland, E. B. Cooper, H. McKittrick, M. Davtian, T. Fong, *J. Sex. Med.* **2012**, *9*, 2868.
[21] J. B. Grubbs, S. L. Perry, J. A. Wilt, R. C. Reid, *Arch. Sex. Behav.* **2019**, *48*, 397.
[22] J. B. Grubbs, C. G. Floyd, K. R. Griffin, T. L. Jennings, S. W. Kraus, *Psychol. Addict. Behav.* **2022**, *36*, 749.
[23] J. B. Grubbs, S. L. Perry, *J. Sex Res.* **2019**, *56*, 29.
[24] K. Lewczuk, I. Nowakowska, K. Lewandowska, M. N. Potenza, M. Gola, *Addiction* **2021**, *116*, 889.
[25] R. L. Solomon, J. D. Corbit, *Psychol. Rev.* **1974**, *81*, 119.
[26] G. F. Koob, M. L.e Moal, *Neuropsychopharmacology* **2001**, *24*, 97.
[27] P. Schulthess, T. M. Post, J. Yates, P. H. van der Graaf, *CPT: Pharmacometrics Syst. Pharmacol.* **2018**, *7*, 111.
[28] R. Gesztelyi, J. Zsuga, A. Kemeny-Beke, B. Varga, B. Juhasz, A. Tosaki, *Arch. Hist. Exact Sci.* **2012**, *66*, 427.
[29] S. Goutelle, M. Maurin, F. Rougier, X. Barbaut, L. Bourguignon, M. Ducher, P. Maire, *Fundam. Clin. Pharmacol.* **2008**, *22*, 633.
[30] D. Mould, R. Upton, *CPT: Pharmacometrics Syst. Pharmacol.* **2012**, *1*, 6.
[31] D. Mould, R. Upton, *CPT: Pharmacometrics Syst. Pharmacol.* **2013**, *2*, 38.
[32] R. N. Upton, D. R. Mould, *CPT Pharmacometrics Syst. Pharmacol.* **2014**, *3*, 88.
[33] T. Chou, M. R. D'Orsogna, *Chaos: Interdiscip. J. Nonlinear Sci.* **2022**, *32*, 021102.
[34] I. Morrison, *Adapt. Hum. Behav. Physiol.* **2016**, *2*, 344.
[35] J. Yim, *Tohoku J. Exp. Med.* **2016**, *239*, 243.
[36] P. M. Topno, D. Thakurmani, Wernicke Encephalopathy: A Case Report, IOSR J. Dent. Med. Sci. **2020**, *19*, 54.
[37] S. H. Ahmed, G. F. Koob, *Psychopharmacology* **2005**, *180*, 473.
[38] E. Agathokleous, M. Kitao, E. J. Calabrese, *Trends Plant Sci.* **2020**, *25*, 1076.
[39] E. J. Calabrese, R. Blain, *Toxicol. Appl. Pharmacol.* **2005**, *202*, 289.
[40] V. Schirrmacher, *Biomedicines* **2021**, *9*, 293.
[41] R. J. Alleman, L. A. Katunga, M. A. M. Nelson, D. A. Brown, E. J. Anderson, *Front. Physiol.* **2014**, *5*, 358.
[42] E. J. Calabrese, *Crit. Rev. Toxicol.* **2008**, *38*, 453.
[43] E. J. Calabrese, *Br. J. Clin. Pharmacol.* **2008**, *66*, 594.
[44] J. L. Prekeges, *J. Nucl. Med. Technol.* **2003**, *31*, 11.
[45] E. J. Calabrese, *Crit. Rev. Toxicol.* **2008**, *38*, 599.
[46] X. Li, T. Yang, Z. Sun, *Trends Endocrinol. Metab.* **2019**, *30*, 944.
[47] A. Mitchell, P. Wei, W. A. Lim, *Science* **2015**, *350*, 1379.
[48] S. J. McMahon, *Phys. Med. Biol.* **2018**, *64*, 01TR01.
[49] M. E. Csete, J. C. Doyle, *Science* **2002**, *295*, 1664.
[50] R. S. Eisenberg, *Nature* **2007**, *447*, 376.
[51] D. B. Newlin, P. A. Regalia, T. I. Seidman, G. Bobashev, in *Computational Neuroscience of Drug Addiction*, (Eds: B. Gutkin, S. H. Ahmed), Springer, New York, NY, **2012**, p. 57.
[52] E. O. Dumas, G. M. Pollack, *AAPS J.* **2008**, *10*, 537.
[53] M. Manojlovich, S. Sidani, *Res. Nurs. Health* **2008**, *31*, 310.
[54] M. A. McVay, G. G. Bennett, D. Steinberg, C. I. Voils, *Health Psychol.: Off. J. Div. Health Psychol. Am. Psychol. Assoc.* **2019**, *38*, 1168.
[55] C. I. Voils, Y. Chang, J. Crandell, J. Leeman, M. Sandelowski, M. L. Maciejewski, *Contemp. Clin. Trials* **2012**, *33*, 1225.
[56] C. I. Voils, H. A. King, M. L. Maciejewski, K. D. Allen, W. S. Yancy, J. A. Shaffer, *Ann. Behav. Med.* **2014**, *48*, 392.
[57] B. Hoza, W. E. Pelham, S. E. Sams, C. Carlson, *Behav. Modif.* **1992**, *16*, 164.
[58] A. Elmokadem, M. M. Riggs, K. T. Baron, *CPT: Pharmacometrics Syst. Pharmacol.* **2019**, *8*, 883.
[59] R. Core Team, **2022**, https://www.R-project.org/.
[60] J. Panksepp, *Affective Neuroscience: The Foundations of Human and Animal Emotions*, Oxford University Press, New York, NY, USA, **1998**.
[61] B. Meibohm, H. Derendorf, *Int. J. Clin. Pharmacol. Ther.* **1997**, *35*, 401.
[62] A. C. Everett, B. E. Graul, J. W. Ronström, J. K. Robinson, D. B. Watts, R. A. España, C. A. Siciliano, J. T. Yorgason, *ACS Chem. Neurosci.* **2022**, *13*, 1534.
[63] G. Bobashev, J. Holloway, E. Solano, B. Gutkin, *A Control Theory Model of Smoking*, RTI Press, USA **2017**, https://doi.org/10.3768/rtipress.2017.op.0040.1706.
[64] M. Luhmann, S. Intelisano, in *Handbook of Well-Being*, (Eds: E. Diener, S. Oishi, L. Tay), DEF Publishers, Salt Lake City, UT **2018**, p. 27.
[65] S. R. J. Maxwell, *Medicine* **2012**, *40*, 351.
[66] R. L. Solomon, *Am. Psychol.* **1980**, *35*, 691.
[67] S. C. Hayes, J. B. Luoma, F. W. Bond, A. Masuda, J. Lillis, *Behav. Res. Ther.* **2006**, *44*, 1.
[68] J. M. Crosby, M. P. Twohig, *Behav. Ther.* **2016**, *47*, 355.
[69] L. Sniewski, P. Farvid, P. Carter, *Addict. Behav.* **2018**, *77*, 217.
[70] M. P. Twohig, J. M. Crosby, *Behav. Ther.* **2010**, *41*, 285.
[71] S. Amigó, A. Caselles, J. C. Micó, *Br. J. Math. Stat. Psychol.* **2008**, *61*, 211.
[72] M. Gårdmark, L. Brynne, M. Hammarlund-Udenaes, M. O. Karlsson, *Clin. Pharmacokinet.* **1999**, *36*, 145.
[73] Y. Levy, D. Levy, A. Barto, J. Meyer, *Front. Psychiatry* **2013**, *4*, 167.
[74] A. Peper, *Pharmacopsychiatry* **2009**, *42*, S1.
[75] C. Porchet, L. Benowitz, B. Sheiner, **1988**, 6.
[76] H. Zou, P. Banerjee, S. S. Y. Leung, X. Yan, *Front. Pharmacol.* **2020**, *11*, 997.
[77] S. M. Shiffman, A. A. Stone, *Technology and Methods in Behavioral Medicine*, Lawrence Erlbaum Associates Publishers, Mahwah, NJ, US, **1998**, pp. 117.
[78] L. P. de Vries, B. M. L. Baselmans, M. Bartels, *J. Happiness Stud.* **2021**, *22*, 2361.
[79] C. Deng, Q. Zhao, R. Shukla, *Hum. Exp. Toxicol.* **2000**, *19*, 703.
[80] S. B. Kim, S. M. Bartell, D. L. Gillen, *Biostatics* **2016**, *17*, 523.
[81] R. Guidry, C. G. Floyd, F. Volk, C. E. Moen, *J. Sex Marital Ther.* **2020**, *46*, 103.
[82] S. Brooks, C. Califf, *Comput. Networks* **2017**, *114*, 143.
[83] J. Bollen, H. Mao, X. Zeng, *J. Comput. Sci.* **2011**, *2*, 1.
[84] A. Dhaoui, S. Bacha, *Cogent Econ. Finance* **2017**, *5*, 1274225.
[85] E. Tuomas, *Int. Society for Music Information Retrieval Conf.* Kobe, Japan, October **2009**.
[86] J. M. Gottman, J. Coan, S. Carrere, C. Swanson, *J. Marriage Fam.* **1998**, *60*, 5.
[87] K. C. Berridge, M. L. Kringelbach, *Neuron* **2015**, *86*, 646.
[88] A. Friedman, M. Frankel, Y. Flaumenhaft, A. Merenlender, A. Pinhasov, Y. Feder, M. Taler, I. Gil-Ad, M. Abeles, G. Yadid, *Neuropsychopharmacology* **2009**, *34*, 1057.
[89] J. Olds, *Sci. Am.* **1956**, *195*, 105.
[90] J. Olds, P. Milner, *J. Comp. Physiol. Psychol.* **1954**, *47*, 419.
[91] K. Solt, C. J. Van Dort, J. J. Chemali, N. E. Taylor, J. D. Kenny, E. N. Brown, *Anesthesiology* **2014**, *121*, 311.
[92] A. M. Fiallos, S. J. Bricault, L. X. Cai, H. A. Worku, M. T. Colonnese, G. G. Westmeyer, A. Jasanoff, *NeuroImage* **2017**, *146*, 1003.

[93] M. Biel, C. Wahl-Schott, S. Michalakis, X. Zong, *Physiol. Rev.* **2009**, *89*, 847.
[94] H.-Y. Chu, Q. Gu, G.-Z. Jin, G.-Y. Hu, X. Zhen, *PLoS One* **2010**, *5*, e13118.
[95] S. Huang, S. L. Borgland, G. W. Zamponi, *Mol. Brain* **2019**, *12*, 89.
[96] A. Momin, H. Cadiou, A. Mason, P. A. McNaughton, *J. Physiol.* **2008**, *586*, 5911.